



RESEARCH ARTICLE

Antibacterial and antifungal effects of *Hippocratea velutina* (Afzel.) leaves and its constituents: Experimental and computational approaches

Akingbolabo Daniel Ogunlakin^{1,*}, Omowumi Temitayo Akinola^{2,*}, Odunayo Victoria Olusegun¹, Dhamodharan Prabhu³, Ahamefula Anslem Ahuchaogu^{4,*}, Amaka Cecilia Agbara⁵, Divine Sokoato Anejukwo¹, Olubunmi Asaleye¹, Oluwadamilola Grace Adedoyin¹, Holiness Balogun¹, Oluwafemi Adeleke Ojo¹, Dare Ezekiel Babatunde⁶, Oluwaseun Abigael Ogunlakin⁷ & Oyindamola Esther Awosola⁸

¹Phytomedicine, Molecular Toxicology and Computational Biochemistry Research Laboratory (PMTCB-RL), Biochemistry Programme, Bowen University, Iwo 232 101, Nigeria

²Microbiology Programme, Bowen University, Iwo 232 101, Nigeria

³Centre for Bioinformatics, Department of Biotechnology, Karpagam Academy of Higher Education, Coimbatore 641 021, Tamil Nadu, India

⁴Department of Industrial Chemistry, Abia State University, Uturu, Nigeria

⁵Department of Chemical Science, Godfrey Okoye University, Enugu, Nigeria

⁶Anatomy Programme, Bowen University, Iwo 232 101, Nigeria

⁷Agricultural sciences programme, Bowen University, Iwo 232 101, Nigeria

⁸Next Era Pharmacy, Lagos, Nigeria

*Correspondence email - g bolaogunlakin@gmail.com, omowumi.akinola@bowen.edu.ng, ahuchaogu.aa@abiastateuniversity.edu.ng

Received: 25 March 2025; Accepted: 17 July 2025; Available online: Version 1.0: 26 August 2025; Version 2.0: 23 September 2025

Cite this article: Ogunlakin AD, Akinola OT, Olusegun OV, Prabhu D, Ahuchaogu AA, Agbara AC, Anejukwo DS, Asaleye O, Adedoyin OG, Balogun H, Ojo OA, Babatunde DE, Ogunlakin OA, Awosola OE. Antibacterial and antifungal effects of *Hippocratea velutina* (Afzel.) leaves and its constituents: Experimental and computational approaches. Plant Science Today. 2025; 12(3): 1-9. <https://doi.org/10.14719/pst.8433>

Abstract

Hippocratea velutina (HV) Afzel's application in wound care suggests its antimicrobial property, although no scientific data confirms its efficacy. Therefore, the antibacterial and antifungal properties of HV leaves are assessed in this study. The methanol extract of HV was evaluated *in vitro* against a variety of bacterial strains, including common fungal pathogens like *Candida albicans* and *Aspergillus niger*, as well as Gram-positive *Staphylococcus aureus*, Gram-negative *Escherichia coli* and Gram-negative *Pseudomonas aeruginosa*. The antimicrobial properties were assessed using agar well diffusion assays. The HPLC-UV-DAD-identified compounds of HV were docked against DNA gyrase from *Bacillus subtilis* and Sterol 14-alpha demethylase from *Aspergillus flavus*. The findings showed that the extract had strong antibacterial and antifungal properties; the inhibition zones for bacterial and fungal strains ranged from 7.0 ± 0.00 to 20.5 ± 4.95 mm and 10.5 ± 0.71 to 12 ± 0.00 mm, respectively, suggesting a broad-spectrum antimicrobial potential. Additionally, the extract demonstrated fungicidal and bactericidal properties at low doses, suggesting its potential as a therapeutic agent. In HV, phenolic compounds such as vitexin and rutin were detected. Sterol 14-alpha demethylase and DNA gyrase showed persistent interactions with rutin and vitexin. These compounds may be working in concert to provide the antimicrobial effects observed. From this study, *Hippocratea velutina* may be a valuable substitute for conventional antimicrobial medicines, with possible uses in the medical and pharmaceutical sectors. It is recommended that further studies be conducted to evaluate its safety, effectiveness and potential for commercialization, including *in vivo* investigations and clinical trials.

Keywords: antimicrobial agent; *Hippocratea velutina*; *in silico* study; rutin; vitexin

Introduction

A diverse group of unicellular microbes, bacteria can be found in almost every environment on Earth, including the human body, soil and water (1). These organisms are classified as prokaryotic, distinguishing them from eukaryotic cells, which lack a distinct nucleus and membrane-bound organelles. Bacteria are highly adaptive and essential to many ecosystems, including human health, despite their basic structure (2). The discovery of new species and variations of well-known bacteria

is ongoing, especially when humans encroach on uncharted environments (3). For instance, *Legionella pneumophila*, which causes Legionnaire's disease and *Borrelia burgdorferi*, which causes Lyme disease, were discovered in the 1970s (4). A greater vulnerability to microbial infections that were previously relatively uncommon has resulted from the growing number of people who are severely immunosuppressed, either as a result of HIV/AIDS or the use of immunosuppressive medications during cancer chemotherapy and organ transplantation (5).

With effects ranging from minor local infections to severe, life-threatening illnesses, bacterial and fungal infections continue to pose significant public health issues on a global scale. Each year, millions of people are afflicted by these infections, which raise morbidity, death and medical expenses. The increasing prevalence of bacterial and fungal infections, particularly those caused by resistant strains, remains a major concern despite advancements in hygiene, diagnostics and treatments. Treatment of these diseases has become more difficult due to the introduction of strains of bacteria and fungi that are resistant to antibiotics and antifungals (6,7). To effectively combat these resistant diseases, it is imperative to investigate alternate therapeutic agents. Botanicals may be a valuable tool in the search for novel antimicrobial drugs, according to a preliminary study that demonstrates the antibacterial properties of natural chemicals and plant extracts (8,9). Furthermore, knowing how these botanicals work may help the scientific community better comprehend antimicrobial and antifungal resistance. This research may lead to the development of combination treatments that enhance therapeutic effectiveness and minimize the risk of resistance development (10). *Hippocratea velutina* Afzel (Celastraceae) is widely distributed in Guinea and Cameroon and is referred to as a "mawolule" by the Yoruba tribe in southwest Nigeria and "dawe" by the Mende people of Sierra Leone (11). Globally, little is known about its ethnobotanical uses. In Nigeria, it is ethnobotanically used to reduce blood glucose levels in diabetic patients, whereas in Sierra Leone, it is frequently used to cure fever and headache (11). *H. velutina* leaves have been shown to have an anti-diabetic effect on albino rats recently (11). Given the rising incidence of infections in immunocompromised individuals, research into this plant's antibacterial and antifungal properties is essential to meeting the urgent demand for effective treatment alternatives against resistant microorganisms. *H. velutina* Afzel's application in wound care in Nigeria suggests that it may have significant impact on a wide range of microorganisms, including fungi and bacteria, improving patient outcomes and developing therapeutic approaches, therefore making a substantial contribution to public health. Hence, this study aims to evaluate the antibacterial and antifungal activities of *H. velutina* leaf and its constituents using *in vitro* and *in silico* methods.

Materials and Methods

Chemicals

Reagents and chemicals of analytical quality were employed in this investigation. The suppliers of all the chemicals employed in this investigation were Aldrich and Chemie GmbH (Steinheim, Germany).

Plant collection and extraction

The Forest Herbarium, Ibadan (FHI) recognized *H. velutina* (HV) leaves that were gathered in Ibadan, Oyo State, Southwest Nigeria. The leaves were ground up and left to air dry. After 14 days of air drying, the leaves were ground into a fine powder using an electric blender. In a covered beaker, 300 g of powdered *H. velutina* leaf material was extracted using 2 L of methanol. For 72 hr, the mixture was left to stand at room temperature. Buchi Rotavapor was used to concentrate the filtrate in vacuo at 40 °C. A refrigerator was used to keep the extracted material.

Antimicrobial assays

Antibacterial study

1g of HV was reconstituted in 30 mL of an aqueous solution to create a solution containing 200 mg/mL of HV. For susceptibility testing, stock solutions of 150 mg/mL, 125 mg/mL and 100 mg/mL were prepared. To create new colonies suitable for the test, bacterial strains were obtained from the Bowen University Microbiology Laboratory, subcultured on nutrient agar plates and then incubated at 37 °C for 24 hr. To guarantee a constant bacterial concentration throughout trials, the bacterial inoculum was standardized using the 0.5 MacFarland standard, which is equivalent to 1.5×10^8 CFU/mL (12). The MHA medium was prepared, sterilized and then transferred into petri plates in a laminar flow hood. A standardized bacterial slurry was applied uniformly to the MHA surface using sterile swabs (13). Using sterile forceps, filter paper discs soaked in HV extract were inserted into the inoculation plates. Gentamicin was used as the positive control and 10 % DMSO as the negative control. Zones of inhibition were measured after incubating for 24 hr at 34 °C (14).

Antifungal testing

1 g of HV was reconstituted in 30 mL of an aqueous solution to create a solution containing 200 mg/mL of HV. For the susceptibility tests, solutions containing 150 mg/mL, 125 mg/mL and 100 mg/mL were made from this stock solution. The fungal strains were then subcultured on SDA plates for 72 hr. The fungal suspension was standardized to the 0.5 MacFarland standard (15). PDA plates were prepared, sterilized and then placed in sterile Petri dishes to solidify. Sterile swabs were used to disseminate the standardized fungal suspension evenly on the SDA plates' surface (16). The inoculated SDA plates were covered with sterilized filter paper discs that had been soaked with HV extract, gentamicin (positive control) and 10 % DMSO (negative control). The plates were incubated for 72 hr at 30 °C (17) and the zones of inhibition were measured.

HPLC-UV-DAD analysis

A quaternary pump and a UV-DAD detector with a C18 column (250 mm × 4.6 mm, internal diameter 5 µm, Zorbax Eclipse Plus, Agilent, USA) were employed in an HPLC system (Agilent Technologies 1100-series, Agilent, San Jose, CA, USA). As per the previously published methodology (18), chromatography was performed using a gradient of H₂O, MeOH and THF. The mobile phase flow rate was 1.5 mL/min and the water was 1 % phosphoric acid (H₃PO₄). The sample was injected in 20 microlitres. Ten minutes were spent purging the column with the mobile phase, 10 min were spent equilibrating and then 35 min were needed for sample analysis. For analysis, spectral data were gathered at a detection wavelength of 220 nm. The compounds were scanned using the DAD detector to determine their MAW and provide further spectral data in the 200-400 nm region. The MAW of each phenolic compound was measured using a variable UV-Vis detector for quantitative purposes, with an external standard. A flow rate of 1.5 mL/min was used to flush the column, which was kept at 30 °C. Comparing retention periods with objective standards and online UV absorption spectrum data was the basis for the compounds' chromatographic identification and validation. Before being injected into an HPLC, the mobile phase was

degassed and all of the produced solutions were filtered through 0.22 µm membranes.

Computational study

Preparation of receptor and ligand molecules for molecular docking

Using the accession numbers P05652 and B8NFL5, respectively, the sequences of DNA gyrase from *Bacillus subtilis* and sterol 14-alpha demethylase from *Aspergillus flavus* were obtained from the UniProt database. Since the macromolecule structure repository, RCSB Protein DataBank, does not contain experimentally confirmed three-dimensional structures, AlphaFold was used to get the protein structures of *A. flavus*' Sterol 14-alpha demethylase and *B. subtilis* DNA gyrase. By altering the bond orders, adding hydrogen atoms, forming disulfide bonds, creating zero-order bonds to metal atoms and generating hetero states, the target proteins' three-dimensional structures were prepared using the Schrodinger Protein Preparation Wizard (19,20). After analyzing the GC/MS analysis hits, the structural coordinates of the 13 compounds that made the shortlist were obtained from the PubChem database. The Schrodinger LigPrep module was used to prepare each of the 13 compounds separately by allocating the appropriate charges and bond orders (21,22). During the ligand production process, a maximum of 32 distinct conformations were created for the phytochemicals. During the preparation process, the OPLS3e force field was used to optimize and minimize the target protein and the compounds.

Molecular docking of compounds and MD simulation of selected top hits

Potential binding sites in the DNA gyrase and Sterol 14-alpha demethylase protein targets were found using the Schrodinger SiteMap module, an effective binding site prediction tool (23,24). With the default settings, Schrodinger's receptor grid creation tool generated a grid surrounding the target proteins' expected binding site (25). The molecular docking procedure, which calculates the binding energy and affinity of the subject compounds with the corresponding targets, was carried out using the Glide XP tool (26). Using Desmond 2021-4, the top-ranked chemicals, Vitexin and Rutin, were separately

simulated bound to the Sterol 14-alpha demethylase and DNA gyrase protein complexes for 500 ns (27). The orthorhombic-shaped TIP3P water model was used to solvate the compound-bound protein complexes. To neutralize the solvated system, we have permitted the program to maintain an adequate concentration of sodium chloride (0.15 M) and counter-ions. Throughout the simulation time, a constant temperature of 300 K and a pressure of 1 atm were maintained. The MD simulation trajectories were periodically recorded and examined using the simulation interaction diagram tool to deduce the behaviour, conformational changes and interactions of bound ligands with their corresponding target proteins.

Statistical analysis

For each study, the investigation was carried out in triplicate and the findings are presented as mean \pm SD, percentages and numbers. Tukey's post hoc test was employed in conjunction with a one-way analysis of variance (ANOVA) to analyze the data. To plot the graphs, we utilized GraphPad Prism 9 edition. A p-value of less than 0.05 is regarded as noteworthy.

Results

Antimicrobial study

Zones of inhibition (ZI) against all bacterial isolates were found to be between 7 ± 0.00 mm and 20.5 ± 4.95 mm in the assay findings (Table 1), while those against fungal isolates were between 10.5 ± 0.71 mm and 13.5 ± 4.95 mm (Table 2).

Phytochemistry and computational study

Molecular docking using the Glide module enabled the observation of interactions, binding properties and binding pocket distances (Table 3). The HPLC chromatogram is shown in Fig. 1. The 2D interactions between rutin and vitexin molecules docked with DNA gyrase and sterol 14-alpha demethylase are shown in Fig. 2. Fig. 3 displays the RMSD of the rutin and vitexin molecules docked against the enzymes DNA gyrase and sterol 14-alpha demethylase. The RMSF of rutin and vitexin molecules docked against sterol 14-alpha demethylase and DNA gyrase is shown in Fig. 4. Fig. S1 shows

Table 1. Antibacterial activities of *Hv* showing zone of inhibition

Bacteria strains	Zone of Inhibition (mm)			
	120 mg/mL	125 mg/mL	150 mg/mL	Control
<i>Pseudomonas aeruginosa</i> (G -ve)	$13.5 \pm 2.12^*$	$11.5 \pm 2.12^*$	$20.5 \pm 4.95^*$	27.0 ± 0.50
<i>Enterobacter</i> species (G -ve)	$10.0 \pm 0.00^*$	$11 \pm 0.00^*$	$7.5 \pm 0.71^*$	17 ± 0.50
<i>Bacillus subtilis</i> (G +ve)	$7 \pm 0.00^*$	$7.5 \pm 0.71^*$	$10.5 \pm 0.71^*$	19 ± 1.41

Data are presented as mean \pm SD, where n = 3. * means significant difference when compared to the control for each microorganism at a p-value of less than 0.05.

Table 2. Antifungal activities of *Hv* showing zone of inhibition

Selected fungi	Zone of Inhibition (mm)			
	120 mg/mL	125 mg/mL	150 mg/mL	Control
<i>Aspergillus flavus</i>	$11 \pm 4.24^*$	$13.5 \pm 4.95^*$	$12 \pm 0.00^*$	19 ± 1.00
<i>Penicillium</i> species	$11.5 \pm 2.12^*$	$11.5 \pm 0.71^*$	$10.5 \pm 0.71^*$	16 ± 1.00

Data are presented as mean \pm SD, where n = 3. * means significant difference when compared to the control for each microorganism at a p-value of less than 0.05.

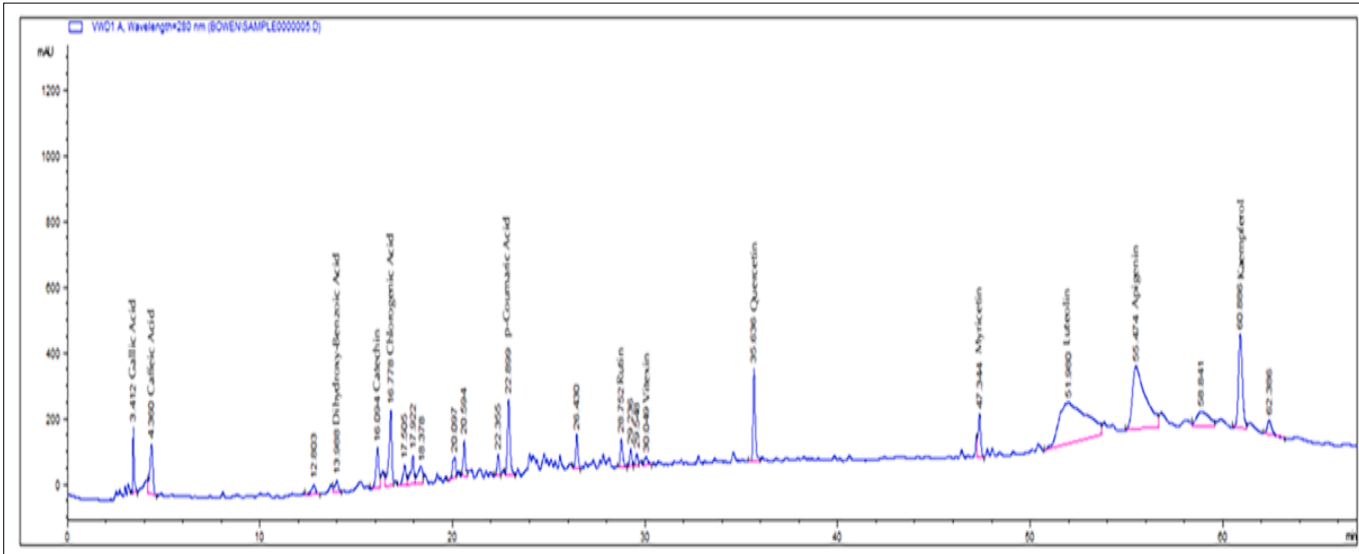


Fig. 1. Chromatogram of *H. velutina* leaf methanol extract.

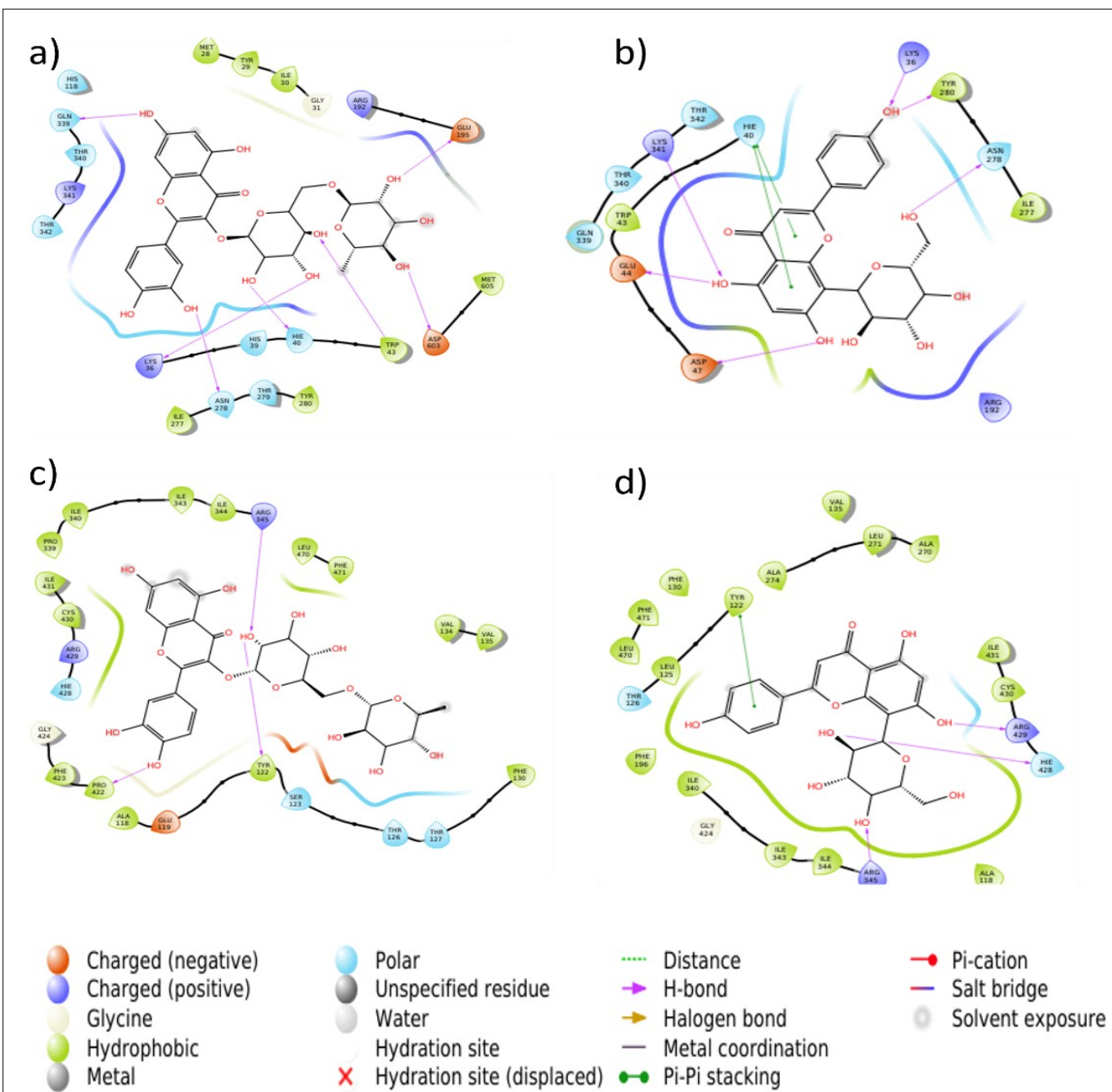


Fig. 2. 2D interactions of (a) Rutin-DNA gyrase, (b) Vitexin-DNA gyrase, (c) Rutin-Sterol 14-alpha demethylase, and (d) Vitexin-Sterol 14-alpha demethylase.

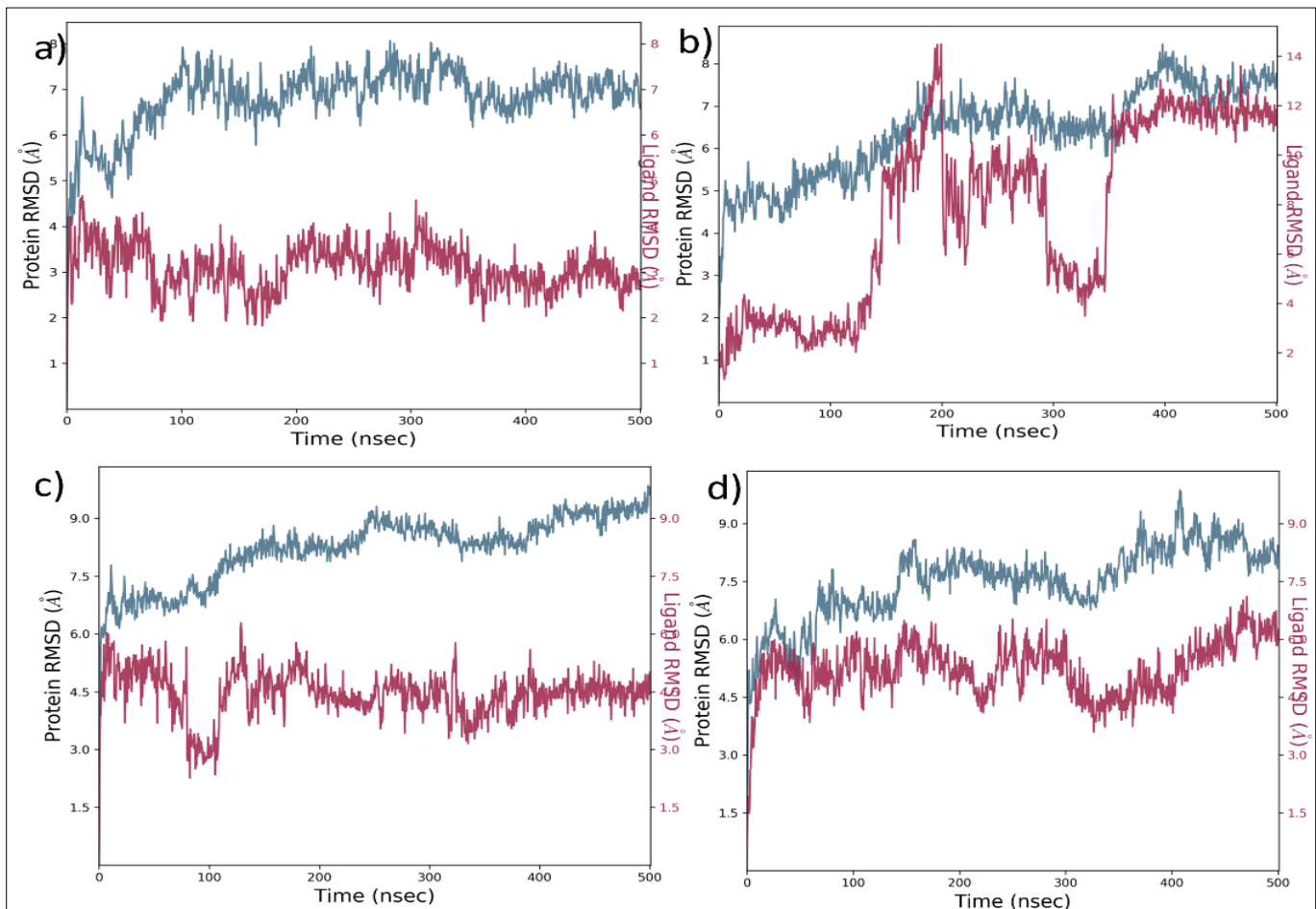


Fig. 3. RMSD of (a) Rutin-DNA gyrase, (b) Vitexin-DNA gyrase, (c) Rutin-Sterol 14-alpha demethylase, and (d) Vitexin-Sterol 14-alpha demethylase interactions.

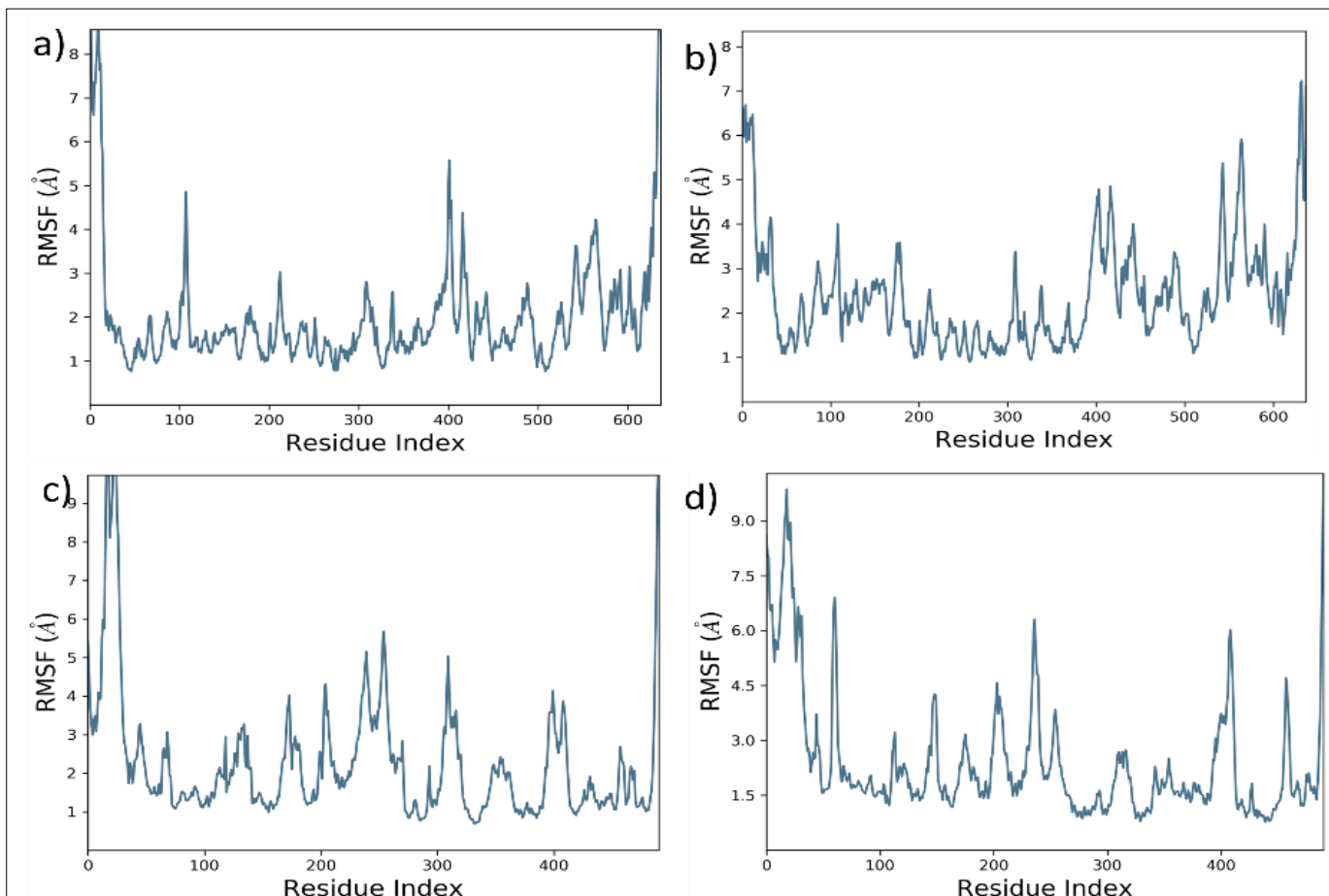


Fig. 4. RMSF of (a) Rutin-DNA gyrase, (b) Vitexin-DNA gyrase, (c) Rutin-Sterol 14-alpha demethylase, and (d) Vitexin-Sterol 14-alpha demethylase interactions.

Table 3. Molecular docking of selective compounds with DNA gyrase from *Bacillus subtilis* and Sterol 14-alpha demethylase from *Aspergillus flavus*

S. No	PubChem ID	Compound Name	Docking Score (kcal/mol)	
			DNA Gyrase	Sterol 14-alpha demethylase
1	370	Gallic Acid	-4.592	-3.922
2	3469	Dihydroxy-benzoic acid	-3.373	-4.766
3	9064	Catechin	-6.646	-6.59
4	637542	P-coumaric acid	-3.731	-4.036
5	689043	Caffeic Acid	-4.39	-3.727
6	1794427	Chlorogenic acid	-6.101	-7.937
7	5280343	Quercetin	-6.944	-7.378
8	5280441	Vitexin	-9.095	-8.139
9	5280443	Apigenin	-6.407	-5.85
10	5280445	Luteolin	-5.753	-6.289
11	5280805	Rutin	-12.81	-10.829
12	5280863	Kaempferol	-6.117	-6.483
13	5281672	Myricetin	-7.007	-7.8

the H-bond interactions of rutin and vitexin molecules docked against sterol 14-alpha demethylase and DNA gyrase.

Discussion

Antimicrobial study

According to the Clinical and Laboratory Standards Institute (CLSI) 2020 guideline for *S. maltophilia*, the zones of inhibition of Hv were significantly larger than the zones of inhibition of every control. The investigation's conclusions show that HV may be a viable antibiotic option, justifying its folkloric use. The activity might be due to the compounds detected in the plant. These compounds include rutin and vitexin. According to research, phenolics and flavonoids contained in medicinal plants provide the building blocks for the creation of antibiotics (28). Bacteria, including *C. frundii*, *E. coli*, *E. aerogenes* and *S. aureus*, are inhibited by crude extracts from *Polygonum persicaria*, *P. plebejum*, *Rumex hastatus*, *R. dentatus*, *R. nepalensis* and *Rheum australe*, which have antibacterial and antifungal qualities (28). Furthermore, preparations from *Calotropis gigantea* have demonstrated strong antifungal efficacy against harmful fungi such as *Aspergillus* species and *Candida albicans* in Asia (29).

The inhibition zone for *P. aeruginosa* increases with concentration of *H. velutina*, peaking at 150 mg/mL. However, even at the highest concentration, the activity remains lower than the control. This suggests the control substance possesses stronger antimicrobial potency against *P. aeruginosa*. Interestingly, the highest concentration of *H. velutina* showed the lowest inhibition against *Enterobacter*. This non-linear trend could imply antagonistic interactions at higher concentrations, instability of active compounds, or resistance mechanisms in *Enterobacter*. Inhibition of *B. subtilis* proliferation improves steadily with concentration of *H. velutina*, though none match the control. This pattern suggests dose-dependent activity, with Gram-positive *B. subtilis* responding more predictably to increasing doses of the compound. Interestingly, the highest concentration of *H. velutina* showed the lowest inhibition of *Enterobacter*. This non-linear trend could imply antagonistic interactions at higher concentrations, instability of active compounds, or resistance mechanisms in *Enterobacter*. Inhibition of *B. subtilis* improves steadily with concentration of *H. velutina*, though none match the control. This pattern suggests dose-dependent activity, with Gram-positive *B. subtilis* responding more predictably to increasing doses. The ethanolic extract from

Plumbago zeylanica root exhibits potent antibacterial activity against *Fusarium equiseti*, *Vibrio cholerae*, *Escherichia coli*, *Pseudomonas aeruginosa*, *Curvularia lunata* and *Colletotrichum corychori* (28). The methanolic leaf extract of *Thevetia peruviana* and the aqueous leaf extracts of *Euphorbia hirta* and *Erythrophleum suaveolens* exhibit antibacterial properties against bacteria that produce extended-spectrum beta-lactamases (ESBLs), such as *Salmonella*, *Proteus*, *Pseudomonas*, *K. pneumoniae*, *E. coli* and methicillin-resistant *Staphylococcus aureus* (MRSA) (29-33). Aqueous and hydroalcoholic extracts from various plants have been found to possess antibacterial properties against multidrug-resistant bacteria, including MRSA and ESBL producers, in a limited study (34).

Phytochemistry and computational study

Binding mode analysis of docked compounds against DNA gyrase and Sterol 14-alpha demethylase

Sterol 14-alpha demethylase proteins were extracted from Alpha Fold for structural study and the 13 chemical molecules that were generated and detected by HPLC analysis were docked into the anticipated active site of DNA gyrase. The compounds' propensity for binding to Sterol 14-alpha demethylase and DNA gyrase was demonstrated by the molecular docking investigation. The chemicals' preventing potential interactions with specific amino acids in the target protein's active site, which are crucial for inhibiting its enzymatic activity. The docking scores of the 13 compounds used in DNA gyrase docking investigations range from -12.81 -- 3.37 kcal/mol. Thirteen compounds, meanwhile, have docking scores ranging from -10.82 - -3.72 kcal/mol. The compounds Rutin and Vitexin have displayed higher affinity computed in terms of docking score among the 13 compounds subjected to binding affinity analysis with DNA gyrase from *B. subtilis* and Sterol 14-alpha demethylase from *A. flavus*. The binding mode analysis of docked complex DNA gyrase with Rutin showed the maximum Glide score of -12.81 kcal/mol with 7 H-bond interactions, the hydroxyl group of compound interacted with Asp603 (C = O...HO; bond length = 2.56 Å), His40 (N...HO; bond length = 2.01 Å), Asn278 (C = O...HO; bond length = 1.75 Å), Lys36 (C = O...HO; bond length = 2.19 Å), Gln339 (C = O...HO; bond length = 1.90 Å), Glu195 (CO....HO; bond length = 1.76 Å) and Trp43 (NH...OH; bond length = 2.45 Å). A Glide score of -9.095 kcal/mol was observed in complex DNA gyrase-Vitexin with one Pi-cation interaction with His40 and 6 H-bond interactions with Lys341 (NH...OH; bond length = 2.23 Å), Glu44 (C = O...HO; bond length = 2.53 Å), Asp47 (CO...HO; 1.73 Å),

Lys36 (NH...OH; 1.98 Å), Tyr280 (HO...OH; bond length=1.88 Å), Asn278 (C=O...HO; bond length = 1.96 Å). The docked complex Sterol 14-alpha demethylase - Rutin showed 3 H-bond interactions with Arg345 (NH...OH; bond length = 2.71 Å), Tyr122 (HO...HO; bond length = 2.10 Å) and Pro422 (C=O...HO; bond length = 2.09 Å) with a Glide score of -10.829 kcal/mol. Three H-bond interactions with Arg429 (C = O...HO; bond length = 1.77 Å), His428 (C=O...HO; bond length=1.78 Å), Arg345 (NH...OC; bond length = 2.01 Å) and one Pi-cation interaction with Tyr122 were observed in complex Sterol 14-alpha demethylase - Vitexin with Glide score -8.139 kcal/mol.

Molecular dynamics simulation of identified compounds bound DNA gyrase and Sterol 14-alpha demethylase complexes

The molecular dynamics simulation technique is used to theoretically study the kinetic movements of biological components, such as proteins and nucleic acids. By reproducing variations in biological molecule configurations across time, atomic-level details about structural alterations are provided by MD modelling. Using MD simulation, the dependability of the ligand molecules within the active site of the proteins DNA gyrase and sterol 14-alpha demethylase was investigated. For the first few nanoseconds, the complexes showed initial variations in the RMSD; however, after the 100 ns simulation, further stability was noted. The complex DNA gyrase-rutin had a maximum RMSD of 8.06 Å at 56 ns, an average of 6.81 Å and a standard deviation of 0.65 Å.

The RMSF was analyzed to identify the interaction of compounds with conformational variations in the complexes. For the complex DNA gyrase - Rutin, higher fluctuations were observed in Met1-Leu16 (range: 10.26 Å - 4.16 Å), Gly108 and Ser109 (range: 4.85 Å and 4.20 Å), Ala401 - Ile404 (range: 5.11 Å - 4.65 Å). For the complex DNA gyrase - Rutin higher fluctuations were observed in Met1 - Leu16 (range: 10.26 Å - 4.16 Å), Gly108 and Ser109 (range: 4.85 Å and 4.20 Å), Ala401 - Ile404 (range: 5.11 Å - 4.65 Å), Lys417 (range: 4.38 Å), Thr565 and Pro566 (range: 4.22 Å and 4.20 Å), Glu627 (range: 4.03 Å), Ala630 - Ile638 (range: 12.93 Å - 4.97 Å). The complex DNA gyrase - Vitexin showed greater fluctuations in Met1 - Leu16 (range: 6.59 Å - 4.11 Å), Thr33 and Asn34 (range: 4.15 Å and 4.07 Å). In complex Sterol 14-alpha demethylase - Vitexin the highly fluctuated residues are Met1 - Val33 (range: 9.86 Å - 4.72 Å), Phe59 - Gly63 (range: 6.90 Å - 4.52 Å), Lys148 - Pro150 (range: 4.26 Å - 4.13 Å), Leu203 - Ala206 (range: 4.56 Å - 4.03 Å), Ala235 - Asp240 (range: 6.30 Å - 4.73 Å), Tyr407 - Leu411 (range: 6.01 Å - 4.25 Å), Gly458 and Val459 (range: 4.70 Å and 4.46 Å), Thr489 - Ala491 (range: 10.25 Å - 5.92 Å). For the complex DNA gyrase - Rutin higher fluctuations were observed in Met1 - Leu16 (range: 10.26 Å - 4.16 Å), Gly108 and Ser109 (range: 4.85 Å and 4.20 Å), Ala401 - Ile404 (range: 5.11 Å - 4.65 Å), Lys417 (range: 4.38 Å), Thr565 and Pro566 (range: 4.22 Å and 4.20 Å), Glu627 (range: 4.03 Å), Ala630 - Ile638 (range: 12.93 Å - 4.97 Å). The complex DNA gyrase - Vitexin showed greater fluctuations in Met1 - Leu16 (range: 6.59 Å - 4.11 Å), Thr33 and Asn34 (range: 4.15 Å and 4.07 Å), Ser109 (range: 4.0 Å), Ser400 - Ser405 (range: 4.78 Å - 4.13 Å), Ser415 - Ser420 (range: 4.85 Å - 4.10 Å), His443 (range: 4.0 Å), Gln542 - Val546 (range: 5.37 Å - 4.0 Å), Lys560 - Pro568 (range: 5.90 Å - 4.35 Å), Ala628 - Ile638 (7.22 Å - 4.52 Å). The residues Met1 and Gly2 (range: 4.52 Å and 5.41 Å), Ser10 (range: 4.0 Å), Glu13 -

Ser30 (range: 11.67 Å - 4.36 Å), Gly174 (range: 4.01 Å), Pro204 and Trp205 (range: 4.23 Å and 4.30 Å), Ser237 - Glu242 (range: 5.14 Å - 4.06 Å), Met252 - Thr257 (range: 5.67 - 4.06 Å), Gly309 - Asp311 (range: 5.02 Å - 4.28 Å), Glu400 (range: 4.12 Å), Val488 - Ala491 (range: 10.82 Å - 5.25 Å) were highly fluctuated in complex Sterol 14-alpha demethylase - Rutin. In complex Sterol 14-alpha demethylase - Vitexin the highly fluctuated residues are Met1 - Val33 (range: 9.86 Å - 4.72 Å), Phe59 - Gly63 (range: 6.90 Å - 4.52 Å), Lys148 - Pro150 (range: 4.26 Å - 4.13 Å), Leu203 - Ala206 (range: 4.56 Å - 4.03 Å), Ala235 - Asp240 (range: 6.30 Å - 4.73 Å), Tyr407 - Leu411 (range: 6.01 Å - 4.25 Å), Gly458 and Val459 (range: 4.70 Å and 4.46 Å), Thr489 - Ala491 (range: 10.25 Å - 5.92 Å).

Protein-ligand interaction profiles were used to measure the degree of binding and we found that the chemicals formed the strongest complex in the target protein's active site through bonding interactions like salt bridges, hydrophobic bonds and hydrogen bonds. In complex DNA gyrase - Rutin, the hydroxyl group of the compound shows hydrogen bond interactions with Glu195 (89 %), Trp43 (97 %), Asn 278 (72 % and 94 %), Tyr280 (33 %), water-mediated hydrogen bond interactions with Leu188 (36 %), His40 (44 %), Lys36 (44 %) and one Pi-cation interaction with His40 (44 %). The complex DNA gyrase-Vitexin shows one hydrogen bond interaction with Glu195 (53 %) and one Pi-cation interaction with Tyr280 (51%). A water-mediated interaction with Ser342 in the complex Sterol 14-alpha demethylase - Rutin. In the complex Sterol 14-alpha demethylase - Vitexin there were 2 Pi-cation interactions with Phe130 (38 %) and Phe196 (50 %), 2 H-bond interactions with Leu125 (33 %), His277 (44 %) and Ile431 (56 %), 3 water mediated H-bond interactions with Val134 (45 % and 48 %) and Arg429 (55 %). The examination of the complexes' RMSD, RMSF and interaction reveals that they are stable in the active sites of the two proteins.

Staphylococcus aureus, *E. coli*, *P. aeruginosa* and *Klebsiella pneumoniae* are among the bacteria that rutin effectively inhibits, including both Gram-positive and Gram-negative strains. When compared to bulk rutin, rutin nanocrystals (RNs) significantly increased antibacterial efficacy, particularly against *P. aeruginosa* and *S. aureus* (35). Increased solubility and bioavailability at the nanoscale were credited with the improvement. Additionally, rutin showed synergistic effects with antibiotics such as amikacin or other flavonoids, lowering the minimum inhibitory concentration (MIC) needed to fight bacteria (36,37). Rutin has shown modest antifungal efficacy, particularly against *Candida albicans*, *Candida krusei* and *Candida gattii* (38). Although effectiveness varies based on concentration and fungus strain, its antifungal mechanism may involve disruption of cell reproduction and modification of membrane permeability (39). Rutin's antifungal efficacy can be enhanced through chemical modifications that alter its steric and hydrophobic properties (40). Furthermore, strong inhibitory effects of vitexin have been shown against methicillin-resistant strains of *S. aureus* (MRSA) (41, 42). Vitexin decreased *S. aureus*'s surface hydrophobicity, which interfered with the production of biofilms and the expression of virulence genes. A derivative of vitexin 2-O-xyloside was discovered to inhibit NorA efflux pumps, increasing the effectiveness of antibiotics against strains of *S. aureus* that are resistant to them (43). When paired with gentamicin or azithromycin, vitexin demonstrated

synergistic antibiofilm actions against *P. aeruginosa* (44). Vitexin has demonstrated modest antifungal activity, particularly against *Aspergillus* species and *C. albicans* (45). Based on the findings of our study, the antimicrobial activity of *H. velutina* may be attributed to the presence of rutin and vitexin. Our findings suggest that the proposed mechanism of action involves inhibition of DNA gyrase and sterol 14-alpha demethylase, thereby disrupting DNA replication in microorganisms and contributing to the plant's bacteriostatic effects.

Conclusion

In *Hippocratea velutina*, phenolic compounds such as vitexin and rutin were detected. Sterol 14-alpha demethylase and DNA gyrase showed persistent interactions with rutin and vitexin. These compounds may be working in concert to provide the antimicrobial effects that have been noted. According to this study, *Hippocratea velutina* may be a promising alternative to antimicrobial traditional drugs, with potential applications in the medical and pharmaceutical sectors. It is recommended that further studies be conducted to evaluate its safety, effectiveness and potential for commercialization, including *in vivo* investigations and clinical trials.

Acknowledgements

We are grateful to the Microbiology programme, at Bowen University for supporting this study.

Authors' contributions

ADO and OTA conceptualized this work. Formal Analysis was done by all authors. ADO, OVO and OTA drafted the manuscript, while revision was done by ADO. ADO and OTA supervised this work.

Compliance with ethical standards

Conflict of interest: The Authors do not have any conflicts of interest to declare.

Ethical issues: None

References

1. Harris C. Bacteria: diversity, classification and significance in ecosystems and human health. *Insight into Epidemiology*. 2024;1(1):1111.
2. Sachdeva S, Sarethy IP. Diving into freshwater microbial metabolites: Pioneering research and future prospects. *Int J Environ Health Res.* 2025;35(2):282–300. <https://doi.org/10.1080/09603123.2024.2351153>
3. McIntyre-Mills JJ. From polarisation to multispecies relationships: re-membering narratives. From polarisation to multispecies relationships: re-generation of the commons in the era of mass extinctions. Singapore: Springer; 2021. p. 173–212. https://doi.org/10.1007/978-981-33-6884-2_10
4. Wright GD. The “molecular logic” underlying antibiotic activity and structure. *Chem Biol.* 2003;10(5):381–2. [https://doi.org/10.1016/S1074-5521\(03\)00105-4](https://doi.org/10.1016/S1074-5521(03)00105-4)
5. Stone M, Bainbridge J, Sanchez AM, Keating SM, Pappas A, Rountree W, et al. Comparison of detection limits of fourth- and fifth-generation combination HIV antigen-antibody, p24 antigen and viral load assays on diverse HIV isolates. *J Clin Microbiol.* 2018;56(8):2045–17. <https://doi.org/10.1128/JCM.02045-17>
6. Kadri SS. Key takeaways from the U.S. CDC's 2019 antibiotic resistance threats report for frontline providers. *Crit Care Med.* 2020;48(7):939–45. <https://doi.org/10.1097/CCM.0000000000004371>
7. Shallcross L, Burke D, Abbott O, Donaldson A, Hallatt G, Hayward A, et al. Factors associated with SARS-CoV-2 infection and outbreaks in long-term care facilities in England: A national cross-sectional survey. *Lancet Healthy Longev.* 2021;2(3):129–42. [https://doi.org/10.1016/S2666-7568\(20\)30065-9](https://doi.org/10.1016/S2666-7568(20)30065-9)
8. Saxena S, Dufosse L, Deshmukh SK, Chhipa H, Gupta MK. Endophytic fungi: A treasure trove of antifungal metabolites. *Microorganisms.* 2024;12(9):1903. <https://doi.org/10.3390/microorganisms12091903>
9. Adesanya EO, Adesanya OO, Ogunlakin AD, Ajayi-Odoko OA, Ojo OA, Odugbemi AI, et al. Antimicrobial activity of *Petivera alliacea* L. root and its constituents: *in vitro* and *in silico* studies. *Vegetos.* 2024;18:1–5. <https://doi.org/10.1007/s42535-024-01085-x>
10. Khodaie L, Patel P, Deore S, Surana V, Byahatti V. Synergistic effects of plant extracts for antimicrobial therapy. In: *Herbal formulations, phytochemistry and pharmacognosy*. Elsevier; 2024. p. 55–76. <https://doi.org/10.1016/B978-0-443-15383-9.00005-6>
11. Oladoja FA, Irokosu ES, Ayoola MD, Elijah OO, Akanji MA, Beatrice OT, et al. Evaluation of the antidiabetic activity and toxicological properties of *Hippocratea velutina* (Afzel.). *Clin Complementary Med Pharmacol.* 2023;3(2). <https://doi.org/10.1016/j.ccmp.2023.100080>
12. Bauer AW, Kirby WM, Sherris JC, Turck M. Antibiotic susceptibility testing by a standardized single disk method. *Am J Clin Pathol.* 1966;45(4):493–6. https://doi.org/10.1093/ajcp/45.4_ts.493
13. The development of the BSAC standardized method of disc diffusion testing. *J Antimicrob Chemother.* 2001;48(1):29–42. https://doi.org/10.1093/jac/48.suppl_1.29
14. Jorgensen JH, Ferraro MJ. Antimicrobial susceptibility testing: A review of general principles and contemporary practices. *Clin Infect Dis.* 2009;49(11):1749–55. <https://doi.org/10.1086/647952>
15. Dwikat M, Amer J, Jaradat N, Salhab A, Rahim AA, Qadi M, et al. *Arum palaestinum* delays hepatocellular carcinoma proliferation through the PI3K-AKT-mTOR signaling pathway and exhibits anticoagulant effects with antimicrobial properties. *Front Pharmacol.* 2023;14:1180262. <https://doi.org/10.3389/fphar.2023.1180262>
16. Arendrup MC, Friberg N, Mares M, Kahlmeter G, Meletiadis J, Guinea J, et al. How to interpret MICs of antifungal compounds according to the revised clinical breakpoints v. 10.0 European committee on antimicrobial susceptibility testing (EUCAST). *Clin Microbiol Infect.* 2020;26(11):1464–72. <https://doi.org/10.1016/j.cmi.2020.06.007>
17. Vanitha PR, Somashekaraiah R, Divyashree S, Pan I, Sreenivasa MY. Antifungal activity of probiotic strain *Lactiplantibacillus plantarum* MYSN7 against *Trichophyton tonsurans*. *Front Microbiol.* 2023;14:1192449. <https://doi.org/10.3389/fmicb.2023.1192449>
18. Araujo-Leon JA, Cantillo-Ciau Z, Ruiz-Ciau DV, Coral-Martinez TI. HPLC profile and simultaneous quantitative analysis of tingenone and pristimerin in four *Celastraceae* species using HPLC-UV-DAD-MS. *Rev Bras Farmacogn.* 2019;29:171–6. <https://doi.org/10.1016/j.bjph.2018.12.009>
19. Release S. 1: Protein Preparation Wizard; Epik, Schrodinger, LLC. Impact, Schrodinger, LLC. 2020.
20. Sundarrajan S, Nandakumar MP, Prabhu D, Jeyaraman J, Arumugam M. Conformational insights into the inhibitory

mechanism of phyto-compounds against Src kinase family members implicated in psoriasis. *J Biomol Struct Dyn.* 2020;38(5):1398–414. <https://doi.org/10.1080/07391102.2019.1605934>

21. Surekha K, Nachiappan M, Prabhu D, Choubey SK, Biswal J, Jeyakanthan J. Identification of potential inhibitors for oncogenic target of dihydroorotate dehydrogenase using *in silico* approaches. *J Mol Struct.* 2017;1127:675–88. <https://doi.org/10.1016/j.molstruc.2016.08.015>
22. Dey D, Kumar A. Structural-based study to identify the repurposed candidates against bacterial infections. *Curr Med Chem.* 2025;32(18):3693–718. <https://doi.org/10.2174/0109298673296749240207115303>
23. Bathula R, Muddagoni N, Lanka G, Dasari M, Potlapally S. Glide docking, autodock, binding free energy and drug-likeness studies for prediction of potential inhibitors of cyclin-dependent kinase 14 protein in Wnt signaling pathway. *Biointerface Res Appl Chem.* 2021;12(2):2473–88. <https://doi.org/10.33263/BRIAC122.24732488>
24. Prabhu D, Rajamanikandan S, Saritha P, Jeyakanthan J. Evolutionary significance and functional characterization of streptomycin adenyltransferase from *Serratia marcescens*. *J Biomol Struct Dyn.* 2020;38(15):4418–31. <https://doi.org/10.1080/07391102.2019.1682046>
25. Rao RG, Biswal J, Dhamodharan P, Kanagarajan S, Jeyaraman J. Identification of potential inhibitors for AIRS from de novo purine biosynthesis pathway through molecular modeling studies – A computational approach. *J Biomol Struct Dyn.* 2016;34(10):2199–213. <https://doi.org/10.1080/07391102.2015.1110833>
26. Broni E, Striegel A, Ashley C, Sakyi PO, Peracha S, Velazquez M, et al. Molecular docking and dynamics simulation studies predict potential anti-ADAR2 inhibitors: implications for the treatment of cancer, neurological, immunological and infectious diseases. *Int J Mol Sci.* 2023;24(7):6795. <https://doi.org/10.3390/ijms24076795>
27. Vyas K, Prabaker S, Prabhu D, Sakthivelu M, Rajamanikandan S, Velusamy P, et al. Study of an inhibitory effect of plant polyphenolic compounds against digestive enzymes using bench-working experimental evidence predicted by molecular docking and dynamics. *Int J Biol Macromol.* 2024;259:129222. <https://doi.org/10.1016/j.ijbiomac.2024.129222>
28. Rahman MS, Anwar MN. Antimicrobial activity of crude extract obtained from the root of *Plumbago zeylanica*. *Bangladesh J Microbiol.* 2007;24:73–5. <https://doi.org/10.3329/bjm.v24i1.1244>
29. Parvin S, Kader MA, Chouduri AU, Rafshanjani MA, Haque ME. Antibacterial, antifungal and insecticidal activities of the n-hexane and ethyl-acetate fractions of methanolic extract of the leaves of *Calotropis gigantea* Linn. *J Pharmacogn Phytochem.* 2014;2(5):47–51.
30. Pacheco AG, Alcantara AF, Abreu VG, Correa GM. Relationships between chemical structure and activity of triterpenes against gram-positive and gram-negative bacteria. In: A search for antibacterials agents. InTech, Rijeka. 2012;1–24. <https://doi.org/10.5772/45649>
31. Chuah E, Zakaria Z, Suhaili Z, Abu Bakar Jamaludin S, Mohd Desa M. Antimicrobial activities of plant extracts against methicillin-susceptible and methicillin-resistant *Staphylococcus aureus*. *J Microbiol Res.* 2014;4:6–13. <https://doi.org/10.1016/j.microbiology.2024040102>
32. Sharifi-Rad J, Mnayer D, Roorintan A, Shahri F, Ayatollahi SAM, Sharifi-Rad M, et al. Antibacterial activities of essential oils from Iranian medicinal plants on extended-spectrum β -lactamase-producing *Escherichia coli*. *Cell Mol Biol.* 2016;62:75–82. <https://doi.org/10.14715/cmb/2016.62.9.12>
33. Niranjan PS, Kaushal C, Jain S. Pharmacological investigation of leaves of *Polyodium decumanum* for antidiabetic activity. *J Drug Deli Ther.* 2017;7(4):69–72. <https://doi.org/10.1016/10.22270/jddt.v7i4.1468>
34. Manso T, Lores M, de Miguel T. Antimicrobial activity of polyphenols and natural polyphenolic extracts on clinical isolates. *Antibiotics (Basel).* 2021;11(1):46. <https://doi.org/10.1016/10.5923/10.3390/antibiotics11010046>
35. Memar MY, Yekani M, Sharifi S, Dizaj SM. Antibacterial and biofilm inhibitory effects of rutin nanocrystals. *Biointerface Res Appl Chem.* 2022;13:132. <https://doi.org/10.33263/BRIAC132.132>
36. Alnour TM, Ahmed-Abakur EH, Elssaig EH, Abduhier FM, Ullah MF. Antimicrobial synergistic effects of dietary flavonoids rutin and quercetin in combination with antibiotics gentamicin and ceftriaxone against *Escherichia coli* (MDR) and *Proteus mirabilis* (XDR) strains isolated from human infections: implications for food-medicine interactions. *Ital J Food Sci.* 2022;34(2):34–42. <https://doi.org/10.15586/ijfs.v34i2.2196>
37. Yi L, Bai Y, Chen X, Wang W, Zhang C, Shang Z, et al. Synergistic effects and mechanisms of action of rutin with conventional antibiotics against *Escherichia coli*. *Int J Mol Sci.* 2024;25(24):13684. <https://doi.org/10.3390/ijms252413684>
38. Oliveira VM, Carraro E, Auler ME, Khalil NM. Quercetin and rutin as potential agents antifungal against *Cryptococcus* spp. *Braz J Biol.* 2016;76(4):1029–34. <https://doi.org/10.1590/1519-6984.07415>
39. Yoruk E. Rutin hydrate induces autophagic cell death and oxidative stress response in phytopathogenic fungus *Fusarium graminearum*. *Zemdirbyste.* 2023;110(4). <https://doi.org/10.13080/z-a.2023.110.042>
40. Prasad R, Prasad SB. A review on the chemistry and biological properties of rutin, a promising nutraceutical agent. *Asian J Pharm Pharmacol.* 2019;5(1):1–20. <https://doi.org/10.31024/ajpp.2019.5.s1.1>
41. Chen Y, Yang J, Huang Z, Yin B, Umar T, Yang C, et al. Vitexin mitigates *Staphylococcus aureus*-induced mastitis via regulation of ROS/ER stress/NF- κ B/MAPK pathway. *Oxid Med Cell Longev.* 2022;2022(1):7977433. <https://doi.org/10.1155/2022/7977433>
42. Das MC, Samaddar S, Jawed JJ, Ghosh C, Acharjee S, Sandhu P, et al. Vitexin alters *Staphylococcus aureus* surface hydrophobicity to obstruct biofilm formation. *Microbiol Res.* 2022;263:127126. <https://doi.org/10.1016/j.mires.2025.128058>
43. Munira S, Zaman SU, Muhit MA. Efflux Pump Inhibitory Potential of Vitexin 2"-O-xyloside Against Gram Positive Bacteria *Staphylococcus aureus*. *Dhaka Univ J Pharm Sci.* 2022;307–15. <https://doi.org/10.3329/dujps.v20i3.59796>
44. Das MC, Sandhu P, Gupta P, Rudrapaul P, De UC, Tribedi P, et al. Attenuation of *Pseudomonas aeruginosa* biofilm formation by vitexin: A combinatorial study with azithromycin and gentamicin. *Sci Rep.* 2016;6(1):23347. <https://doi.org/10.1038/srep23347>
45. Al-Otibi FO, Alrumeizan GI, Alharbi RI. Evaluation of anticandidal activities and phytochemical examination of extracts prepared from *Vitex agnus-castus*: a possible alternative in treating candidiasis infections. *BMC Complement Med Ther.* 2022;22(1):69. <https://doi.org/10.1186/s12906-022-03552-x>

Additional information

Peer review: Publisher thanks Sectional Editor and the other anonymous reviewers for their contribution to the peer review of this work.

Reprints & permissions information is available at https://horizonpublishing.com/journals/index.php/PST/open_access_policy

Publisher's Note: Horizon e-Publishing Group remains neutral with regard to jurisdictional claims in published maps and institutional affiliations.

Indexing: Plant Science Today, published by Horizon e-Publishing Group, is covered by Scopus, Web of Science, BIOSIS Previews, Clarivate Analytics, NAAS, UGC Care, etc. See https://horizonpublishing.com/journals/index.php/PST/indexing_abstracting

Copyright: © The Author(s). This is an open-access article distributed under the terms of the Creative Commons Attribution License, which permits unrestricted use, distribution and reproduction in any medium, provided the original author and source are credited (<https://creativecommons.org/licenses/by/4.0/>)

Publisher information: Plant Science Today is published by HORIZON e-Publishing Group with support from Empirion Publishers Private Limited, Thiruvananthapuram, India.